

Physicochemical characteristics of glycerol-plasticized dextran/soy protein isolate composite membranes

Surabhi Singh, Bhuvanesh Gupta

Bioengineering Laboratory, Department of Textile Technology, Indian Institute of Technology, New Delhi 110016, India

Correspondence to: B. Gupta (E-mail: bgupta@textile.iitd.ernet.in)

ABSTRACT: This work deals with the preparation and characterization of *in situ* crosslinked dextran/soy protein isolate composite membranes as a function of increasing glycerol content. The surface morphology of the membranes, as evidenced from field emission scanning electron microscopy and atomic force microscopy, exhibited smoother surfaces with increasing glycerol content up to 30%. The wettability, color, and UV-blocking characteristics of the membranes were studied. The glycerol content also significantly influenced the water vapor transmission rate of the membranes, demonstrating diminishing membrane permeability with increasing glycerol content. In addition, the membranes presented an increase in water vapor loss up to 5 h with glycerol content ranging from 10% to 30%, whereas a decrease in vapor loss has been elucidated with 40% glycerol. The influence of plasticization on the rheological properties of the composite fluid was investigated. Although the tensile strength and modulus decreased with increasing glycerol content up to 30%, a significant increase was observed beyond this due to the antiplasticizing effect of glycerol that is dominant at concentrations higher than 30%. A structural analysis of the membranes using attenuated total reflectance indicates an increase in the intensity of the —OH stretching region with increasing glycerol content. Further, X-ray diffraction patterns showed a decrease in crystalline behavior up to 30% glycerol content, above which the antiplasticizing effect of glycerol was dominant. © 2016 Wiley Periodicals, Inc. *J. Appl. Polym. Sci.* **2016**, *133*, 43847.

KEYWORDS: biocompatibility; biomedical applications; biopolymers & renewable polymers; composites; structure–property relations

Received 22 February 2016; accepted 24 April 2016

DOI: 10.1002/app.43847

INTRODUCTION

Polysaccharide–protein complexes have been the subject of rising interest in the field of biopolymer-based hybrid materials.^{1,2} Polysaccharides possess reactive functional groups that covalently conjugate to proteins at high temperatures of ~70–90 °C, which is dependent on the Amadori rearrangement of the naturally occurring Maillard reaction.^{3–7} Glycosylation occurring between the reducing end group of dextran and the amine of soy protein isolate (SPI) has attracted considerable attention due to its potential to overcome issues related to the solubility, mechanical properties, and synthesis/degradation ratio of SPI.⁸ Dextran is an intriguing biomaterial due to its biocompatible, biodegradable, and nontoxic nature and has evolved as a fascinating hydrogel for wound regeneration.^{9,10} Soy protein too has attracted considerable attention in the area of wound healing as it promotes rapid cell proliferation.¹¹ Polysaccharide-based membrane development for wound dressing applications has been suggested as one of the essential formulations in the area of healthcare applications; however, cast dry membranes and films based on dextran exhibit fragile tensile characteristics.^{12,13} This induces difficulty in obtaining unified dextran membranes,

causing inconvenience during practical applications. Extensive research has been dedicated to the advantages of *in situ* crosslinking in the dextran–SPI system for the food industry, but its efficiency in the form of membranes for integrated healthcare with favorable mechanical strength, as well as overcoming the toxicity problems of external crosslinkers, needs to be explored.

To enhance the flexibility and handling properties of biopolymer films, various plasticizers, usually polyols, have been extensively employed. Because of the enormous number of hydroxyl groups present in glycerol, it is the most preferred hydrophilic plasticizer for water-soluble polysaccharides and is used to overcome brittleness in films by reducing the intermolecular forces existing between long chains of proteins, leading to an increase in mobility of the polymer chains and obtaining films with improved flexibility.^{14–16} It has been reported that starch-based materials manifest poor mechanical properties and reduced elongation in ambient situations.¹⁷ Consequently, the incorporation of a plasticizer, such as glycerol or sorbitol, helps in the reduction of its brittleness. Plasticizers also affect the water vapor permeability rate as well as the mechanical properties of any biomaterial.^{18,19}

Table I. Composition of Dextran, SPI, and Glycerol in D/SPI/G Membranes

Dextran (%)	Soy protein isolate (%)	Glycerol (%)
54	36	10
48	32	20
42	28	30
36	24	40

In our previous work, we adopted a novel strategy to develop bioresource-based dextran/SPI/glycerol (D/SPI/G) composite membranes with varying SPI content, where glycerol was fixed in all compositions.²⁰ The optimized concentration of the D/SPI/G membranes was found to be 42/28/30. After SPI, glycerol served as the second most essential component to produce plasticized flexible membranes. Also, an appropriate reinforcing effect of SPI in dextran membranes was visualized. Their structure–property relationships were extensively investigated using various chemical and spectroscopic techniques and were shown to be strongly dependent on the SPI content.

In the present work, a comprehensive examination of mechanical properties, water vapor transmission rate, and microstructural properties of the resulting composite membranes as a function of varying concentrations of glycerol will be elucidated. The synthesis route for the membranes has already been reported in our previous publication.²⁰ These membranes are subsequently projected for application in wound care management.

EXPERIMENTAL

Materials

Dextran ($M_w \sim 70,000$ kD) was procured from Sigma Chemicals (Bengaluru, India). Glycerol was supplied by Fisher Scientific (Pune, India), and soy protein isolate (92% pure) was purchased from Nutrimed Healthcare Limited (New Delhi, India). Millipore water was used for the filmogenic solutions.

Plasticization of D/SPI System with Glycerol

The procedure for the preparation of D/SPI/G membranes has been described in detail in our previous work.²⁰ Briefly, a dextran solution was prepared in deionized water under stirring. Subsequently, SPI powder was added to the dextran solution, followed by glycerol addition. In the present work, a 2% polymer solution was prepared with appropriate amounts of glycerol (10–40% G) under constant stirring for 48 h at 70 °C. At the end of the reaction, the solutions were poured onto polypropylene petri dishes and then dried at 70 °C for 2 days to produce air-dried plasticized membranes. The weight-based percentage compositions of the membranes are presented in Table I.

Characterization

Field Emission Scanning Electron Microscopy. The membranes were dried under vacuum and fractured using liquid nitrogen. The fractured specimens were then mounted on a sample stage, keeping the fractured surfaces pointed upward with the help of conductive tape. The samples were sputter-coated with a thin layer of gold using a Hitachi E 1010 Ion Sputter coating machine (Hitachi, Tokyo, Japan). The morphology of the D/SPI/G membranes was examined by a Hitachi

S4800 field emission scanning electron microscope (FESEM) operated at 3 kV. The magnification was maintained at 2500× and 10,000×.

Atomic Force Microscopy. The surfaces of the dried D/SPI/G membranes were imaged by tapping mode under ambient conditions by a Solver Pro SPM (NT–MDT, Moscow, Russia) atomic force microscope (AFM) with NSG 10 series tips. Surface topographical information was obtained at a scanning frequency of 0.5 Hz by a silicon nitride cantilever. Root mean square (RMS) roughness (S_q) was measured at three different locations on each film with the scanning size of each image kept at 20 μ × 20 μ.

Color Measurements. The color of the control (without glycerol) and plasticized membranes was determined according to the International Commission on Illumination (CIE) scale. Three measurements around the membranes were performed to obtain color values l^* (luminosity), a^* (red–green), b^* (yellow–blue), and c^* (chrome). A white standard color plate was used for calibration and as background. The total color difference was calculated using eq. (1)²¹:

$$\Delta E^* = \{(\Delta l^*)^2 + (\Delta a^*)^2 + (\Delta b^*)^2\}^{1/2} \quad (1)$$

where $\Delta l^* = l^* - l_0^*$, $\Delta a^* = a^* - a_0^*$, and $\Delta b^* = b^* - b_0^*$, where l_0^* , a_0^* , and b_0^* represent color values for the control membranes (without glycerol), and l^* , a^* , and b^* represent the color values for glycerol-plasticized membranes.

UV Protection Factor. The UV protection factor (UPF) values of membranes at five different locations were assessed using a Labsphere UV-100 F Ultraviolet Transmission Analyzer (North Sutton, NH) according to standard AATCC 183:2004.

Tensile Strength. Tensile tests were performed on an Instron Microtensile Tester, Model 5848, Singapore, equipped with a 10 N load cell. The thickness of the samples was measured using a thickness meter at five random positions. Preconditioned film samples were cut into rectangular strips of 10 mm width and 30 mm length and mounted between the grips of the equipment for testing. A crosshead speed of 50 mm/min at 27 ± 2 °C and 50 ± 2% relative humidity were the operating conditions for the instrument. The elastic modulus and the ultimate elongation of the films were obtained from the stress–strain curves. The data representation is of the samples evaluated in triplicate.

Moisture Absorption. To investigate the effect of glycerol on the wettability of D/SPI/G membranes, the sessile drop method was adopted. The contact angle formed on the surface of the membranes by a drop of deionized water was measured using Rame goniometer model 100-00-230 (Succasunna, NJ). All measurements were performed at a constant temperature, and the procedure was repeated three times.

Determination of Gel Content. The D/SPI/G membranes were cut into 2 × 2 cm² pieces, dried in a vacuum oven at 50 °C for 8 h, and then weighed. After drying, the initial weight of each sample (W_1) was determined on a precision balance. Films of varying glycerol content were kept in a phosphate buffer of pH 7.4 for 24 h in a shaking water bath. After 24 h, the insoluble crosslinked fraction was separated from the noncrosslinked part that gets dissolved in the PBS. The latter represents the weight



Figure 1. Pictorial representation of D/SPI/G membranes with glycerol content (10–40%). [Color figure can be viewed in the online issue, which is available at wileyonlinelibrary.com.]

loss in the membranes. The extracted membranes were then dried in a vacuum oven at 60 °C for 5 h to obtain the residual weight (W_2). The calculation for the exact gel content was carried out according to eq. (2):²⁰

$$\text{Gel content (\%)} = \frac{W_2}{W_1} \times 100 \quad (2)$$

Swelling Studies. The swelling studies of the D/SPI/G membranes were conducted at 37 °C and pH 7.4 using a phosphate-buffered saline (PBS) buffer. The initial dry weight of all samples (M_1) was kept equal to understand the effect of glycerol loss on equilibrium swelling. The membranes were taken out of the buffer solution at predetermined time intervals and weighed after removing the excess water on the surfaces with the help of filter paper. The equilibrium swelling degree was determined using eq. (3):

$$\text{Equilibrium swelling (\%)} = \frac{M_2 - M_1}{M_1} \times 100 \quad (3)$$

where M_1 is the weight of the dry membrane and M_2 is the equilibrium weight of the swollen membrane.

Rheology Studies. Shear viscosity measurements of the pristine dextran, pristine SPI, and polymer composites were performed using an Anton Paar MCR702 rheometer (Anton Paar, Graz, Austria) at a shear rate of 0.1 s⁻¹ to 1000 s⁻¹. The temperature in the measurements was kept constant at 30 °C.

Water Vapor Transmission Rate. Water permeability measurements across the membranes were carried out according to the ASTM method E398-03. The water vapor transmission rate

(WVTR) was determined using an automatic Lyssy L80-5000 (PBI Dansensor, Ringsted, Denmark) water vapor permeability tester. The measurements were recorded at 38 °C and 10–15% relative humidity by placing the membrane over an aluminum sample card.

Attenuated Total Reflectance. Attenuated total reflectance (ATR) spectra of the D/SPI/G membranes with varying glycerol content were recorded using a Perkin Elmer Spectrum-BXFTIR system (Waltham, MA). The scanning of samples was performed in the range 400–4000 cm⁻¹ at a resolution of 2 cm⁻¹.

X-ray Diffraction. X-ray diffraction (XRD) patterns were obtained using a wide-angle PANalytical X'Pert PRO instrument (Netherlands) operating at 40 mA and 40 kV using sealed-tube Cu K α radiation.

RESULTS AND DISCUSSION

Visualization of D/SPI/G Membranes

The D/SPI/G membranes prepared with 2% polymer concentration exhibited improved handling features and appearance in comparison to those with 1% concentration; this was due to enhanced polymeric interactions, as shown in previous work.²⁰ Glycerol has a profound influence on the integrity of the membranes. The photomicrographs in Figure 1 indicate that the membrane without glycerol presents more irregular, rigid and brittle features. However, films with 30% and 40% glycerol exhibited a smoother and continuous surface that can be attributed to the enhanced polymer–plasticizer interactions among polymer chains, consequently leading to better membrane

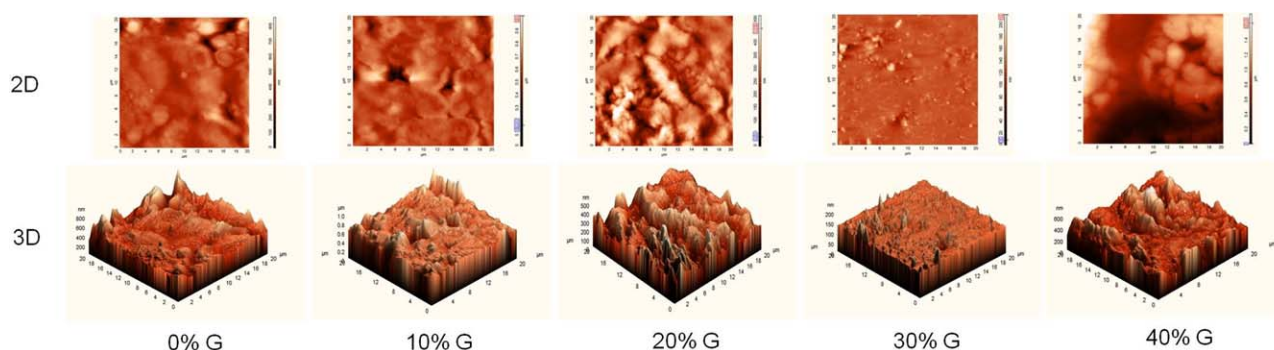


Figure 2. AFM images of D/SPI/G membranes depicting surface roughness with glycerol concentration (10–40%). [Color figure can be viewed in the online issue, which is available at wileyonlinelibrary.com.]

flexibility. At lower glycerol concentration, a nonhomogeneous distribution of glycerol within the membranes was responsible for the rugged surface, indicating that a glycerol content less than 20% does not produce an effective plasticizing effect, which can help in producing flexible membranes with a continuous matrix.

Surface Topographical and Morphological Analysis of Membranes

The surface of the D/SPI/G membranes was monitored by AFM to evaluate their morphology and porosity with increasing glycerol content (Figure 2). Membranes without glycerol showed a root mean square (rms) roughness of 72.4 nm, while for 10% glycerol the film surface showed higher rms roughness (78.3 nm) because of the aggregated structures formed, with some protrusions resulting from the phase-coarsening effect taking place with the addition of glycerol. Moreover, the surface was covered with a large number of small pores that contributed to high roughness. No distinguishable variations in the roughness up to 20% glycerol were observed with an rms roughness of 76.6 nm, whereas a distinct and prominent change occurred at 30% glycerol, where a drastic reduction in surface roughness produced an rms value of 8.5 nm. The results were consistent with the values presented in our previous work for the membranes prepared with 1% polymer solution and with

30% glycerol.²⁰ It can be proposed that membranes with 30% glycerol exhibited smoother zones possibly generated by the incorporation of the short plasticizer chains, leading to the formation of more homogeneous zones. This can be attributed to the fact that the formation of large glycerol-rich domains help in minimizing the phase-coarsening effect, resulting in a noticeable even and dense dispersion of regular globular structures without protuberances. Moreover, the protrusions were found to be interconnected, forming a dense, smooth structure. Glycerol has the capacity to influence the roughness factor and the aggregation behavior of D/SPI/G membranes. A further increase in glycerol content over 30% leads to no major difference in the rms roughness value, but a slight increase was due to the anti-plasticizing effect causing modifications in the material integrity because of the extremely high glycerol content.^{22–24} This postulation is supported by the tensile results in a subsequent section.

Changes in morphology of the membranes after the addition of glycerol were further supported by the FESEM analysis, as depicted in Figure 3. Both D/SPI/G samples with 10% and 20% glycerol revealed some protuberances on the surfaces of the membranes. This may be due to redundant glycerol molecules being aggregated in the films. However, as the glycerol content increases to 30%, the membranes display smoother surfaces,

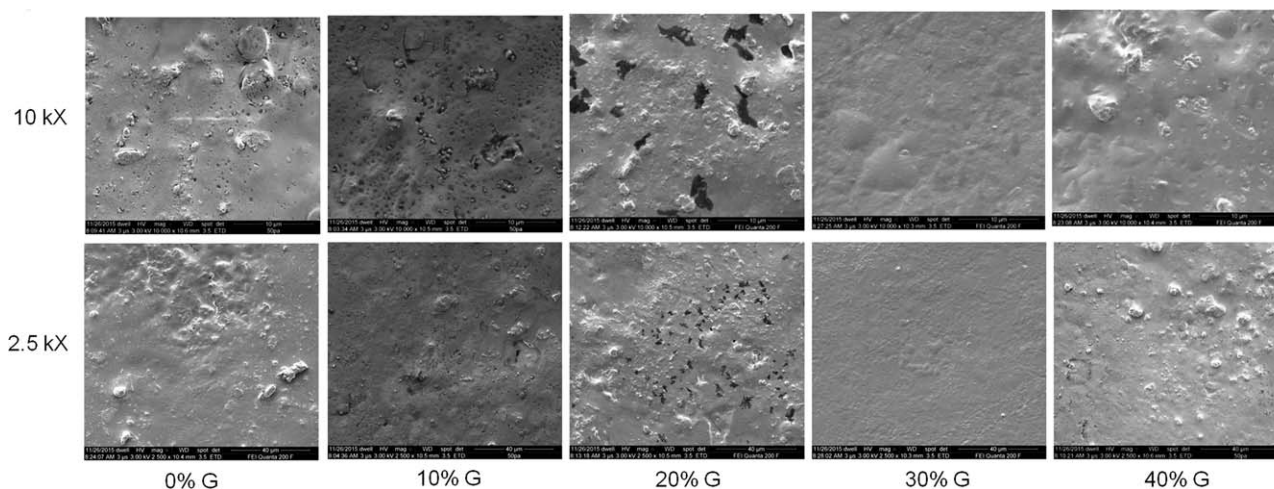


Figure 3. FESEM images of D/SPI/G membranes with glycerol content (0–40%).

Table II. Color Values of Control Membrane and Glycerol-Plasticized Membranes

Sample designation	L^*	a^*	b^*	c^*	ΔE^*
Control	40.57 ± 0.05	0.18 ± 0.005	1.38 ± 0.025	1.39 ± 0.025	NA
10% G	53.33 ± 0.40	2.17 ± 0.035	17.55 ± 0.12	17.64 ± 0.13	16.66 ± 0.35
20% G	51.73 ± 0.57	0.89 ± 0.065	13.67 ± 0.02	13.69 ± 0.01	20.60 ± 0.15
30% G	45.76 ± 0.38	0.82 ± 0.04	11.86 ± 0.04	11.91 ± 0.03	11.84 ± 0.14
40% G	39.98 ± 0.41	1.17 ± 0.05	11.29 ± 0.76	11.40 ± 0.78	10.05 ± 0.80

which is a direct implication of glycerol being homogeneously distributed in the entire region. A slight roughness is again noticed with a high glycerol content of 40%, complementing the results presented in the AFM analysis.

Color and UPF of Membranes

The color parameters (L^* , a^* , b^* , c^* color values) and total color difference (ΔE^*) of the D/SPI films at different plasticizer contents are presented in Table II. The addition of glycerol to D/SPI-based membranes showed a significant increase in L^* (lightness/darkness) and indicated an increase in the membrane lightness. Furthermore, an intense yellowness has been noted with a significant increase in b^* values with respect to the control sample, indicating a pronounced Maillard reaction that is due to a higher reducing end content in the system.^{21,25} Also, the total color difference decreased with the glycerol addition.

The effectiveness of plasticized membranes against harmful UV rays was analyzed, and the UPF values are presented in Table III. The membrane with 0% glycerol was too brittle to be analyzed for its UPF value. It has been reported that materials having a UPF of 50 or greater exhibit excellent UV protection.²⁶ Taking this into account, all membranes displayed remarkable UV-blocking properties. High UPF values might be attributed to the presence of SPI in the system, as peptides are known to be natural UV absorbers.²⁷ The difference in UPF values can be due to the location and extent of distribution of components in the matrix.

Effect of Glycerol Content on Hydrophilicity of Membranes

The change in the hydrophilic nature of the membranes was investigated using contact-angle measurements (Figure 4). We noticed a pronounced decrease in the initial contact angle by increasing the glycerol content. Membranes with 0% glycerol were too brittle to be placed flat on the substrate for contact-angle analysis. Glycerol is highly sensitive to relative humidity due to the presence of hydroxyl groups in it. Consequently, the presence of plasticizer makes the membrane surface more hydrophilic. Likewise, there is an increase in the surface polarity of the films.¹⁵ As a result, when a water droplet is placed on the

Table III. UPF Values of D/SPI/G Membranes at Different Glycerol Concentrations

Sample designation	UPF
10% G	249.97 ± 36.57
20% G	284.29 ± 14.94
30% G	298.36 ± 18.02
40% G	225.22 ± 46.11

film surface, a force of attraction between the water molecules and the film surface comes into play. A lower contact angle corresponds to a strong attraction between the two.

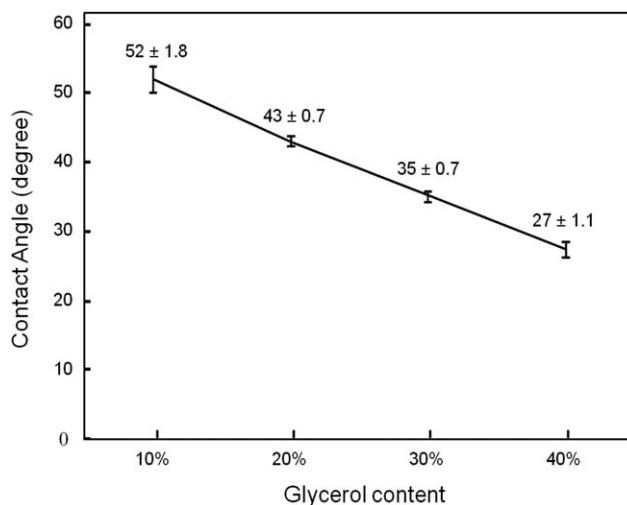
Additionally, SPI molecules contribute to enhancing the hydrophilicity as they are randomly coiled proteins that have the ability to reorganize the distribution of hydrophilic moieties present at the surface, whereas hydroxyl groups are located on sugar rings in dextran, thus possessing less freedom to rearrange themselves.

Gel Content in Membranes

The variation of gel content with glycerol content is presented in Figure 5. The gel content decreases with an increase in glycerol content in the membranes. This trend seems to be due to the cumulative loss of uncrosslinked gel and glycerol, which increases as the glycerol content increases. Taking into account the glycerol content in each membrane and its complete elimination from the matrix, it may be suggested that the fraction of the gel that is crosslinked is not affected by the glycerol content in the membranes. If we can determine that glycerol completely leached out of the matrix, it may be proposed that a fraction of D/SPI in the range of 18–24% is lost, which seems to be almost identical for all membranes.

Swelling Studies

Water uptake of the membranes is shown in Figure 6. It can be seen that the equilibrium swelling of D/SPI/G membranes decreases from 322% to 117% when the glycerol content increases from 10% to 40%. Membranes with 0% glycerol were too brittle

**Figure 4.** Effect of glycerol content on the hydrophilicity of D/SPI/G membranes.

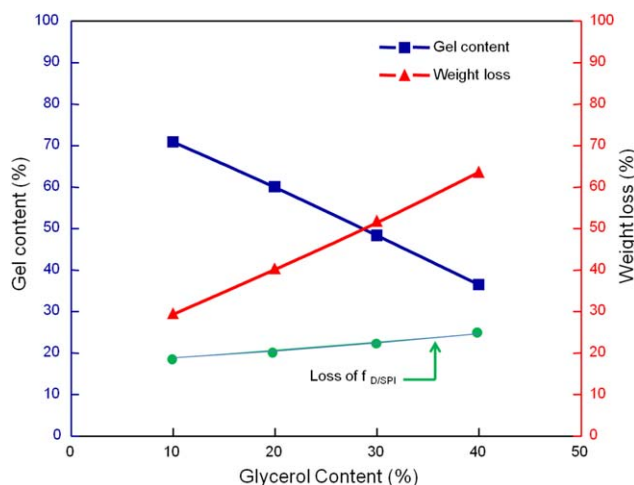


Figure 5. Gel content, weight loss, and fractional loss of D/SPI in D/SPI/G membranes with glycerol content (10–40%). [Color figure can be viewed in the online issue, which is available at wileyonlinelibrary.com.]

to be handled for the swelling analysis. As depicted in Figure 5, the weight loss in the membranes is predominantly due to the loss of glycerol, which further determines the fraction of D/SPI that governs the swelling of membranes in PBS. The highest weight loss was observed in the membrane with 40% G (Figure 5), resulting in a small fraction of D/SPI remaining for swelling, in comparison to those with 10%, 20%, and 30% glycerol.

Rheology

The rheological properties of pristine and composite fluids are shown in Figure 7. During the measurements, the shearing action caused the molecules to rotate, giving rise to sinusoidal forces and resulting in alternating stretching and compression of the molecules, which was further influenced by the extent of plasticization in the system. A continuous decrease in shear viscosity with shear rate of the D/SPI/G composite fluid has been observed with an increase in glycerol concentration, thus displaying the shear-thinning behavior of a non-Newtonian composite fluid.^{28,29} This observed pseudoplastic behavior might be attributed to the

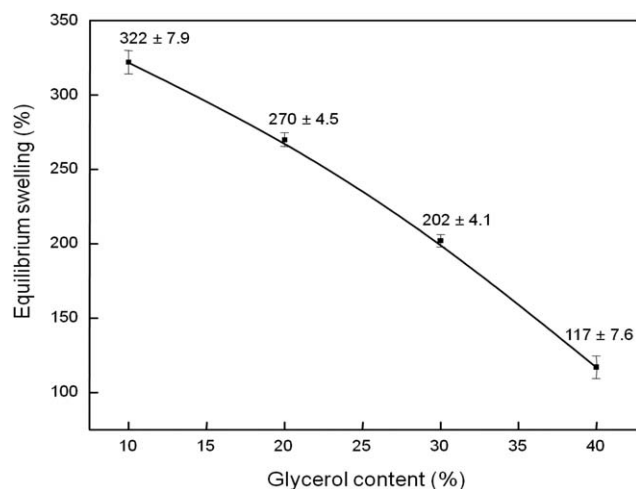


Figure 6. Equilibrium swelling of D/SPI/G membranes with glycerol content (10–40%).

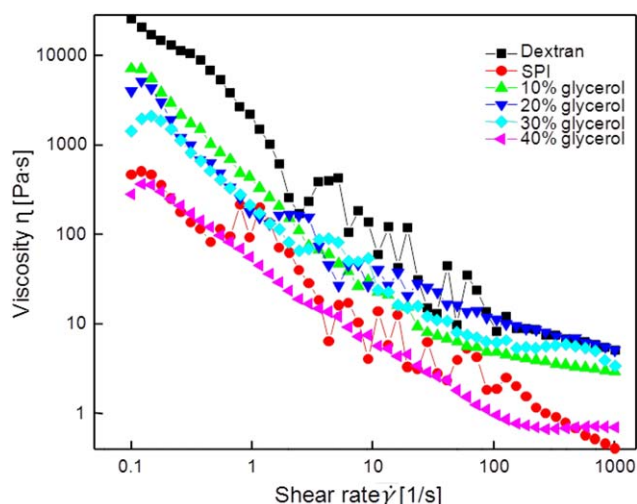


Figure 7. Effect of glycerol plasticization on the shear viscosity of D/SPI/G composite fluid with glycerol content (10–40%). [Color figure can be viewed in the online issue, which is available at wileyonlinelibrary.com.]

strong plasticization in the system causing a decrease in the intermolecular forces between the D/SPI chains, thus leading to an increase in chain mobility and a decrease in viscosity.

Attenuated Total Reflectance

The ATR spectra of the membranes with varying glycerol content are represented in Figure 8. Broad absorption peaks in the range 3200–3600 cm^{-1} were associated with the stretching vibration of hydroxyl (OH) groups of the dextran unit as well as glycerol. The band obtained at 2920 cm^{-1} was assigned to C–H stretching in the dextran molecule. The band at 1150 cm^{-1} corresponds to the glycosidic bridge and valent vibrations of the C–O–C bond in dextran, whereas valent vibrations of C–C are associated with the band at 1107 cm^{-1} . The band located at 1000 cm^{-1} refers to the deformational vibrations of the C–O–H bond. Further, pristine SPI presented

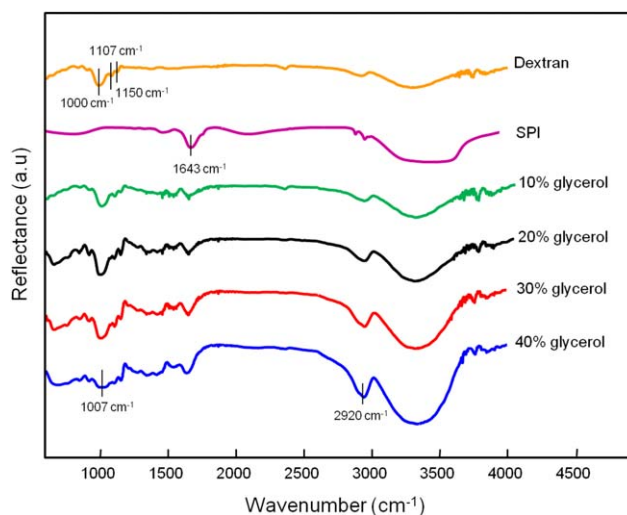


Figure 8. ATR spectra of pristine dextran, pristine SPI, and D/SPI/G membranes with glycerol content (10–40%). [Color figure can be viewed in the online issue, which is available at wileyonlinelibrary.com.]

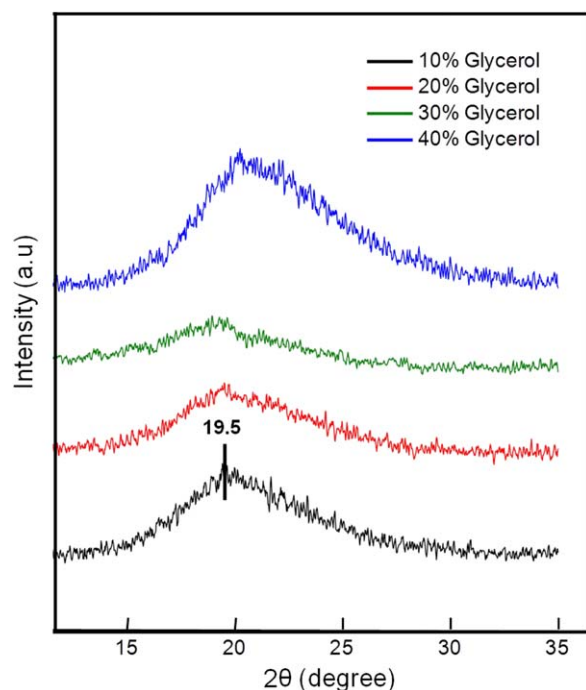


Figure 9. Diffractograms of D/SPI/G membranes with glycerol content (10–40%). [Color figure can be viewed in the online issue, which is available at wileyonlinelibrary.com.]

a peak around $1640\text{--}1650\text{ cm}^{-1}$ related to the amide bond in the SPI unit that was absent in dextran. NH stretching occurs in the region of $3100\text{--}3300\text{ cm}^{-1}$, which is difficult to observe as the band is fused with the OH stretching of dextran. The addition of glycerol is evident by the increase in the intensity of the peaks associated with OH stretching at higher glycerol content, which leads to an increase in the intermolecular hydrogen bonding. Slight differences in band intensity or shape or a shift in a peak can be attributed to changes taking place in the level of hydrogen bonding in the system and new interactions that have arisen between glycerol and the D/SPI matrix. The peak at 1000 cm^{-1} related to C—O—H bond vibrations exhibited a shift to 1007 cm^{-1} , which can be due to changes from the amorphous to the crystalline state in the polymer.

X-ray Diffraction

The XRD patterns of the D/SPI/G membranes at different glycerol contents are presented in Figure 9. In our previous work, a broad peak of dextran was observed at 18.8° , indicating its amorphous nature,²⁰ whereas the characteristic peaks of SPI were obtained around 19.5° . According to the diffractograms for composite membranes, the intensity of the peaks decreased with increasing glycerol content up to 30%, though the peak position was almost similar. This shows that a high amount glycerol incorporation did not produce any major alterations in the diffraction pattern but reduced the crystallinity level, as glycerol possesses a highly amorphous character, which resulted in an increase in the level of amorphousness in the polymer. Glycerol addition blocked the reorganization of D/SPI units and restricted the growth of crystalline domains on nuclei by forming strong hydrogen bonding with the hydroxyl groups of dextran. A sharp

increase in crystalline behavior with 40% glycerol was due to the antiplasticizing effect of glycerol that increased the crystallinity.

Tensile Studies

Tensile properties are of key importance in apprehending the effect of glycerol on the performance of this polymer composite, as it assists in providing an insight into the influence of molecular packing on membrane handling and durability. To examine the effect of glycerol on the strength, flexibility, and stability of D/SPI/G membranes, tensile studies were performed, and the results are shown in Figure 10. D/SPI/G films without glycerol were too brittle to be handled to determine their tensile properties. The addition of glycerol altered the mechanical properties of the membranes because of its highly hydrophilic nature. Tensile strength (TS) and Young's modulus (YM) results are elaborated in Table IV. Elongation at break was found to increase from 16.3% to 31% with an increase in the glycerol content up to 30% because of the plasticizing effect of glycerol. Similar behavior has also been observed in starch–chitosan films, where the tensile loss takes place as the glycerol content increases.³⁰

However, a disparate trend was observed with 40% glycerol where elongation at break was reduced to 18.3%, probably ascribable to the antiplasticizing effect caused by the presence of a high amount of glycerol in the system, which has already been proved by other authors as well.^{22–24} An antiplasticization-dominated mechanism is a result of strong interactions between glycerol and the polymer that cause loss of mobility within the macromolecular chains. In addition, the membrane with 10% glycerol exhibited higher TS and maximum load (ML) than the ones with 20% and 30% (Table IV, Figure 10), due to structural changes taking place with the increasing effect of plasticization. Likewise, membranes with 30% glycerol manifested the highest

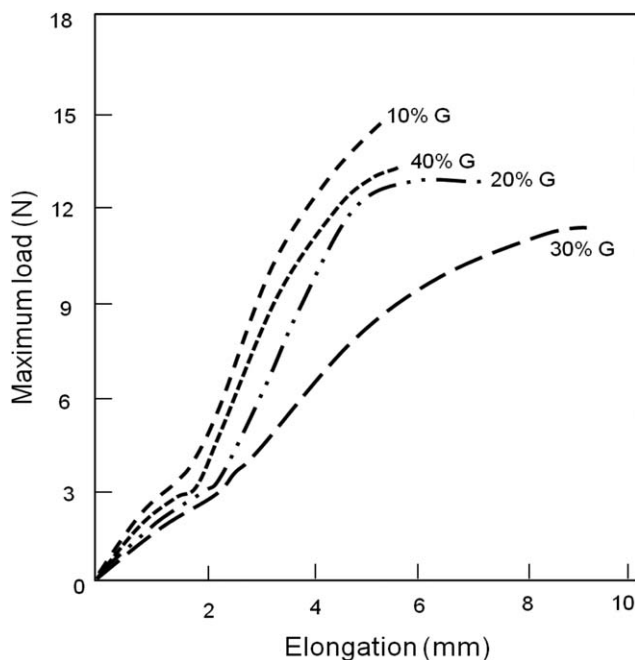


Figure 10. Load-displacement curves of glycerol-plasticized D/SPI/G membranes under tensile stress. Gauge length 30 mm; strain rate 50 mm min^{-1} ; load cell 10 N.

Table IV. Effect of Glycerol Content on the Tensile Properties of D/SPI/G Membranes

Glycerol content	Elongation at break (%)	Tensile strength (MPa)	Young's modulus (MPa)
10%	16.3 ± 0.08	6.5 ± 0.13	65.5 ± 2.52
20%	23 ± 0.13	5.7 ± 0.04	55.9 ± 0.26
30%	31 ± 0.02	4.5 ± 0.03	44.2 ± 0.28
40%	18.3 ± 0.04	6.1 ± 0.03	77.8 ± 3.84

Gauge length 30 mm; strain rate 50 mm min⁻¹; load cell 10 kg.

reduction in bonds between the dextran chains, allowing greater flexibility and consequently decreasing the TS and YM to 4.5 MPa and 44.2 MPa, respectively. Furthermore, a distinctive increase in both TS and ML with 40% glycerol was again a direct indication of the antiplasticizing effect, which deteriorates tensile properties. A reduction in flexibility of the membranes (40% G) due to pronounced antiplasticization resulted in a significant increase in modulus to 77.8 MPa, inducing rigidity and making the membranes stiffer. The results were comparable with the surface morphology pattern observed in the AFM and SEM images.

Water Vapor Transmission Rate

Glycerol, being a low-molecular-weight substance, results in a disruption of intermolecular interaction among polymer chains by penetrating the protein network. It can even be apprehended that the plasticization changes the mobility of chains, facilitating the diffusion process since structural changes in the membranes are affected. The study of the WVTR provides enlightenment into vapor transfer mechanisms and interactions between polysaccharide and protein chains in the membrane, which are further influenced by factors such as the hydrophilic nature of the polymer, the presence of pores, and the tortuosity of pathways inside the membrane.³¹ WVTR helps in determining the moist environment in a wound, which plays a pivotal role during the

process of wound healing. An optimum value of WVTR is very essential, as very high WVTR can cause water loss at a rapid rate, leading to dehydration at the wound site by the interruption of cellular migration and tissue repair, making peeling painful. On the other hand, if WVTR is too low, it can lead to exudate retention, thus raising chances of wound infection. Commercially used wound dressings like Medihoney HCS, Tegaderm hydrocolloid, Duoderm Fignal, Nu-Gel, and Aquacel have WVTR values of approximately 600–650 g/m²/day, 300–400 g/m²/day, 100–150 g/m²/day, 850–950 g/m²/day, and 400–470 g/m²/day, respectively,³² while island dressing has a very high WVTR of 9540 g/m²/day. It is noteworthy that most of the available dressings either possess a very low or a very high WVTR, causing problems during the healing process.³²

Parameters like porosity and thickness of membranes greatly influence the WVTR. Dextran, possessing a great number of hydrophilic groups, leads to higher interaction with water molecules, which further enhances the permeation of water vapor. An ideal wound dressing material should have the ability to control water loss from a wound at a favorable rate with minimum risk of dehydration. The membranes in the present investigation showed a value ranging from 2376 g/m²/day to 4312 g/m²/day, which is close to the range adequate for maintaining fluid balance at the wound site, as shown in Figure 11. The WVTR decreased with increasing the glycerol content, possibly because of the formation of hydrogen bonds between the hydroxyl groups of glycerol and dextran, which results in the consumption of free sorption sites available for water molecules in glycerol-plasticized membranes, also reported by a few authors.^{33–35} In addition, it can also be attributed to the incorporated amorphous glycerol moieties within the dextran/SPI matrix that impede the diffusion rate of water vapor from the bulk matrix.

The water vapor loss from the membranes over specific time intervals was calculated to determine their efficacy for use during prolonged periods. It was observed that water vapor loss increases up to 5 h for membranes with 10%, 20%, and 30% glycerol content. After 5 h, the membrane with 30% glycerol showed a maximum water vapor loss of approximately 43%, which decreased slowly to about 39% over 10 h. Conversely, membranes with 40% glycerol showed a distinguishable trend where a linear decrease in the vapor loss up to 10 h was observed. The pattern of water vapor loss with glycerol content was observed over three time intervals. It was seen that loss of the water attached to the hydrophilic groups of glycerol and dextran takes place over 5 h, after which there was a decrease in percent water vapor loss that is due to bound water molecules. Subsequently, there was no water loss from the membranes, and the membrane with 30% glycerol retained a minimum amount of bound water. From this study it was clear that the material will lose its water content when exposed to air over extended periods. Thus, it can be suggested that this conjugate material can be more suitable at wound sites with exudates rather than dry wounds.

CONCLUSIONS

In this work, nonbrittle glycerol-plasticized D/SPI/G composite membranes were prepared using a solvent casting process. The

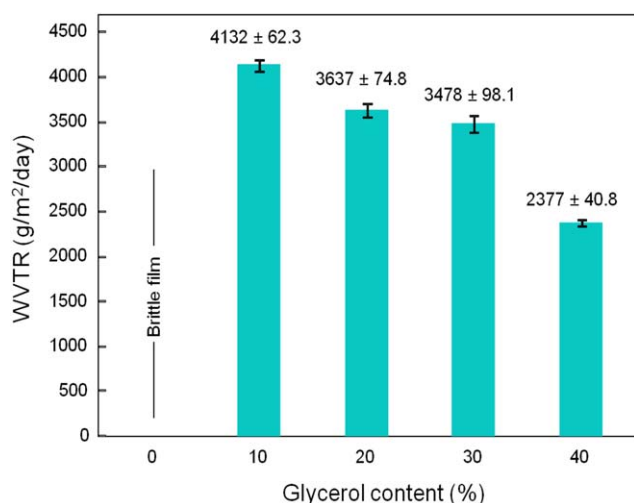


Figure 11. Water vapor transmission rate in D/SPI/G membranes with glycerol content (10–40%). [Color figure can be viewed in the online issue, which is available at wileyonlinelibrary.com.]

results obtained emphasize that plasticization due to glycerol introduces flexibility into the D/SPI/G membranes, thus ameliorating their handling characteristics. Glycerol-free films were brittle and were not characterized further. Therefore, morphological changes, water vapor transmission properties, and tensile properties were evaluated for plasticized membranes at distinct glycerol contents. The morphology and topography of membranes were found to improve up to 30% glycerol, whereas at 40% glycerol ruggedness was observed. A detailed analysis of tensile properties showed that at glycerol contents higher than 30% the membranes exhibited declined flexibility due to an antiplasticizing effect becoming dominant at glycerol contents higher than 30%. The membranes showed excellent resistance to UV light, and the total color difference (ΔE^*) was found to decrease with the glycerol addition. The membranes displayed excellent WVTR, which was found to decrease with the increase in glycerol content. Also, an increase in water vapor loss from the membranes was seen up to 5 h with glycerol content ranging from 10% to 30%. The hydrophilic behavior of the membranes became more pronounced with increasing glycerol content, as confirmed by the contact-angle analysis. Further, the glycerol content also influenced the weight loss in the membranes, and the results suggested that the higher the plasticizer content, the higher was the weight loss due to leaching out of glycerol, whereas the loss in fraction of D/SPI was found to be in the range of 18–24%, which appeared to be almost identical for all membranes. Equilibrium swelling of membranes and viscosity of the composite fluid decreased with increasing glycerol content. Glycerol addition was apparently observed by the increase in the intensity of peaks associated with OH stretching by spectroscopic analysis. Furthermore, an antiplasticizing effect of glycerol was also observed in the diffraction pattern of membranes with more than 30% glycerol content, as shown by a sharp increase in crystalline behavior.

ACKNOWLEDGMENTS

The authors are extremely grateful to the Indian Institute of Technology, Delhi, India for providing research funds.

REFERENCES

1. Ibrahim, B. A.; Kadum, K. M. *Mod. Appl. Sci.* **2010**, *4*, 157.
2. Liu, L. S.; Kost, J.; Yan, F.; Spiro, R. C. *Polymers* **2012**, *4*, 997.
3. Zhuo, X. Y.; Qi, J. R.; Yin, S. W.; Yang, X. Q.; Zhu, J. H.; Huang, L. X. *J. Sci. Food Agr.* **2013**, *93*, 316.
4. Li, X.; Cheng, Y.; Yi, C.; Hua, Y.; Yang, C.; Cui, S. *Food Hydrocolloids* **2009**, *23*, 1015.
5. Diftis, N.; Kiosseoglou, V. *Food Hydrocolloids* **2004**, *18*, 639.
6. Diftis, N.; Kiosseoglou, V. *Food Chem.* **2006**, *2*, 228.
7. Diftis, N. G.; Biliaderis, C. G.; Kiosseoglou, V. D. *Food Hydrocolloids* **2005**, *19*, 1025.
8. Miralles, B.; Martinez-Rodriguez, A.; Santiago, A.; van de Lagemaat, J.; Heras, A. *Food Chem.* **2007**, *100*, 1071.
9. Sun, G.; Shen, Y. I.; Kusuma, S.; Fox-Talbot, K.; Steenbergen, C. J.; Gerecht, S. *Biomaterials* **2011**, *32*, 95.
10. Unnithan, A. R.; Barakat, N. A.; Pichiah, P. B.; Gnanasekaran, G.; Nirmala, R.; Cha, Y. S.; Jung, C. H.; El-Newehy, M.; Kim, H. Y. *Carbohydr. Polym.* **2012**, *90*, 1786.
11. Egozi, D.; Baranes-Zeevi, M.; Ullmann, Y.; Gilhar, A.; Keren, A.; Matanes, E.; Berdicevsky, I.; Krivoy, N.; Zilberman, M. *Burns* **2015**, *41*, 1459.
12. Schmid, M. *Materials* **2013**, *6*, 3254.
13. Vieira, M. G. A.; da Silva, M. A.; dos Santos, L. O.; Beppu, M. M. *Eur. Polym. J.* **2011**, *47*, 254.
14. Jouki, M.; Khazaei, N.; Ghasemlou, M.; Hadinezhad, M. *Carbohydr. Polym.* **2013**, *96*, 39.
15. Ramos, O. L.; Reinas, I.; Silva, S. I.; Fernandes, J. C.; Cerqueira, M. A.; Pereira, R. N.; Vicente, A. A.; Pocas, M. F.; Pintado, M. E.; Malcata, F. X. *Food Hydrocolloids* **2013**, *30*, 110.
16. Colak, B. Y.; Gouanve, F.; Degraeve, P.; Espuche, E.; Prochazka, F. J. *Membr. Sci.* **2015**, *478*, 1.
17. Laohakunjit, N.; Noomhorm, A. *Starch-Starke* **2004**, *56*, 348.
18. Ghasemlou, M.; Khodaiyan, F.; Oromiehie, A.; Yarmand, M. S. *Int. J. Biol. Macromol.* **2011**, *49*, 378.
19. Andrade-Mahecha, M. M.; Tapia-Blacido, D. R.; Menegalli, F. C. *Carbohydr. Polym.* **2012**, *88*, 449.
20. Singh, S.; Gupta, B. *Polym. Bull.* **2016** (submitted for publication).
21. Leceta, I.; Guerrero, P.; de la Caba, K. *Carbohydr. Polym.* **2013**, *93*, 339.
22. Lourdin, D.; Bizot, H.; Colonna, P. *J. Appl. Polym. Sci.* **1997**, *63*, 1047.
23. Souza, A. C.; Benze, R.; Ferrão, E. S.; Ditchfield, C.; Coelho, A. C. V.; Tadini, C. C. *LWT-Food Sci. Technol.* **2012**, *46*, 110.
24. Shimazu, A. A.; Mali, S.; Grossmann, M. V. E. *Semina: Ciências Agrárias, Londrina*, **2007**, *28*, 79.
25. Noronha, C. M.; deCarvalho, S. M.; Lino, S. M.; Barreto, P. L. *Food Chem.* **2014**, *159*, 529.
26. Vijayalakshmi, D.; Ramachandran, T. *IJFTR* **2013**, *38*, 309.
27. Korac, R. P.; Khambholja, K. M. *Pharmacogn. Rev.* **2011**, *5*, 164.
28. Zepnik, S.; Kabasci, S.; Kopitzky, R.; Hans-Joachim, R.; Wodke, T. *Polymers* **2013**, *5*, 873.
29. Zepnik, S.; Kabasci, S.; Kopitzky, R.; Hans-Joachim, R.; Wodke, T. *J. Mater. Sci. Eng. A* **2012**, *2*, 152.
30. Liu, F.; Qin, B.; He, L.; Song, R. *Carbohydr. Polym.* **2009**, *78*, 146.
31. Yoshida, C. M. P.; Junior, E. N. O.; Franco, T. T. *Packag. Technol. Sci.* **2009**, *22*, 161.
32. Derma Sciences Europe Ltd., U.K. Medihoney® in Hydrogel Dressing with Super Absorbent Polymer. Available at: http://jmvprod.weebly.com/uploads/1/7/0/3/17038090/medihoney_hcs.pdf (Accessed February 20, 2016).
33. Boonsong, P.; Laohakunjit, N.; Kerdchoechuen, O.; Tusvil, P. *Int. Food. Res. J.* **2009**, *16*, 97.
34. Farahnaky, A.; Saberi, B.; Majzoobi, M. J. *Texture Stud.* **2013**, *44*, 176.
35. Parra, D. F.; Tadini, C. C.; Ponce, P.; Lugao, A. B. *Carbohydr. Polym.* **2004**, *58*, 475.